

## Accepted Manuscript

Title: Decontamination of radioactive metal surfaces by electrocoagulation

Authors: Alberto A. Pujol Pozo, Erika Bustos Bustos, Fabiola Monroy-Guzmán



PII: S0304-3894(18)30748-9  
DOI: <https://doi.org/10.1016/j.jhazmat.2018.08.061>  
Reference: HAZMAT 19685

To appear in: *Journal of Hazardous Materials*

Received date: 1-9-2017  
Revised date: 1-8-2018  
Accepted date: 19-8-2018

Please cite this article as: Pujol Pozo AA, Bustos Bustos E, Monroy-Guzmán F, Decontamination of radioactive metal surfaces by electrocoagulation, *Journal of Hazardous Materials* (2018), <https://doi.org/10.1016/j.jhazmat.2018.08.061>

This is a PDF file of an unedited manuscript that has been accepted for publication. As a service to our customers we are providing this early version of the manuscript. The manuscript will undergo copyediting, typesetting, and review of the resulting proof before it is published in its final form. Please note that during the production process errors may be discovered which could affect the content, and all legal disclaimers that apply to the journal pertain.

# Decontamination of radioactive metal surfaces by electrocoagulation

Alberto A. Pujol Pozo<sup>1,2</sup>, Erika Bustos Bustos<sup>2</sup>, Fabiola Monroy-Guzmán<sup>1,\*</sup>

<sup>1</sup>Instituto Nacional de Investigaciones Nucleares.

Carretera México-Toluca S/N, La Marquesa, Ocoyoacac, Edo. de México, C. P. 52750,  
México

<sup>2</sup>Centro de Investigación y Desarrollo Tecnológico en Electroquímica, S. C.

Parque Tecnológico s/n Sanfandila, Pedro Escobedo, Querétaro. C. P. 76703, México.

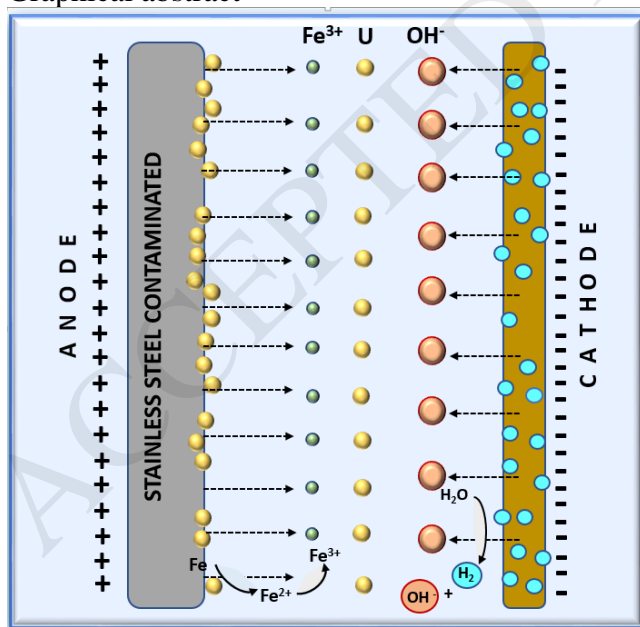
apujol@cideteq.mx ; ebustos@cideteq.mx ; fabiola.monroy@inin.gob.mx

Corresponding author

\*Tel: +52 (55) 53.29.72.00 ext 3400

fabiola.monroy@inin.gob.mx (Fabiola Monroy-Guzman)

Graphical abstract



## HIGHLIGHTS

- It is feasible to apply the electrocoagulation (EC) process to decontaminate steel contaminated with U.
- Contaminated metal is used as the sacrificial anode and the cathode Ti.
- Decontamination efficiency depends on geometry, dimensions and surface conditions of the metal.
- The grease or dust presence on the metal surface reduces the treatment efficiency.
- Iron hydroxides formed in the EC process carry U to the sludges.

## ABSTRACT

The decontamination of noncompactable radioactive wastes, such as tools and equipment, aims to reduce the waste volume to be conditioned and stored. The electrocoagulation (EC) application in the decontamination of noncompactable radioactive waste from stainless steel containing uranium, was studied to evaluate its technical viability. The first studies were carried out with stainless steel plates coated with  $\text{WO}_3$  to simulate a fixed contamination and to determine the best tungsten removal conditions by EC considering pH, electrolyte support, distance between the electrodes, cell potential and counter-electrode material. The best removal conditions for  $\text{WO}_3$  were applied to plates contaminated with  $\text{UO}_2(\text{NO}_3)_2$  to evaluate the viability of the EC decontamination process. Uranium removal efficiencies of 90% were obtained in 1 h, at pH of 1, 2.4 V and 1 cm of distance between anode / cathode in a circular array. The EC process, under the previously obtained conditions, was applied to two metallic pieces contaminated with U. It proved feasible to decontaminate metallic pieces through the EC process, thus being able to obtain up to 90% U removal efficiency; however, it is important that the surfaces of the parts are free of grease and dust.

**KEYWORDS:** uranium, electrocoagulation, decontamination, radioactive metal surfaces

## 1. Introduction

Radioactive waste management aims to prevent the dispersion of radioisotopes into the biosphere. Within the management of radioactive wastes of noncompactable materials, such as equipment and tools, treatment techniques focusing on their decontamination are used to reduce waste volume by removing the radionuclides present in the materials. Surface contamination in these wastes can be in the form of layers of oxides, adhered muds, salts or fats. The radioactive contamination forms part of these layers, and, when removed by decontamination techniques, radionuclides are also removed from these materials. The selection of treatments or different decontamination routes depends on the characteristics of the material to be decontaminated, such as composition, size, type of contamination and final use of the decontaminated material: reclassification, reuse or release as conventional waste [1].

Electrochemical methods, such as electrocoagulation (EC), can be applied in the decontamination of small-size stainless steel parts of simple geometries that have fixed contamination. In principle, the pieces are immersed in solutions, and a potential difference is applied. These decontamination methods are efficient and generate low volumes of secondary waste [2]. Electrocoagulation is a process of destabilizing water pollutants through the action of low-voltage direct electric current and metal sacrificial electrodes, usually aluminum/iron [3], where a high ion charge is generated electrochemically to destabilize the contaminants present.

In this work, the feasibility of the electrocoagulation process to decontaminate stainless steel containing uranium on its surface was studied. For this purpose, preliminary tests were carried out on stainless steel specimens contaminated with tungsten (W) in order to determine the conditions for the treatment of steel contaminated with uranium (U), considering that tungsten has chemical properties analogous to U. The decontamination treatment developed using the steel probes coated with W was finally applied to metal parts contaminated with U, classified as noncompactable radioactive waste, contaminated with U.

## **2. Experimental**

### **2.1. Preparation of stainless steel test pieces**

Steel probes (SS alloy 304) of  $2.5 \times 5$  cm were used as working electrodes, sanded on both sides, immersed in ethyl alcohol for 2 min, dried at room temperature for 1 day and finally weighed. These electrodes were coated with  $\text{WO}_3$ ,  $^{187}\text{WO}_3$  or  $\text{UO}_2(\text{NO}_3)_2$  dissolved in a

polyacrylate emulsion (EPA) to simulate a fixed contamination on the surface of the stainless steel plates [4]. The mixture of tungsten-polyacrylate oxide (W-EPA) was prepared with 1 g of  $\text{WO}_3$  in 3.5 mL of EPA plus 200  $\mu\text{L}$  of  $\text{H}_2\text{O}_2$  at 70 °C with constant stirring. The  $^{187}\text{WO}_3$ -polyacrylate ( $^{187}\text{W-EPA}$ ) blend was made with 100 mg of  $^{187}\text{WO}_3$  (1.8  $\mu\text{Ci} / \text{mg}$ ) in 3.5 mL of EPA and 200  $\mu\text{L}$  of  $\text{H}_2\text{O}_2$  at 70 °C. The uranyl-polyacrylate nitrate (U-EPA) mixture was prepared with 100  $\mu\text{L}$  of 0.21 M  $\text{UO}_2(\text{NO}_3)_2$  with a specific activity of 1.32 KBq / mL and the same volume of EPA and  $\text{H}_2\text{O}_2$  as used for W-EPA. The test pieces (working electrodes) were coated using the painting technique and allowed to dry at room temperature.

## 2.2. Quantification of W, W-187 and U in electrochemical tests

The determination of  $\text{WO}_3$  during the electrochemical process was performed by UV-Vis spectrophotometry on a Perkin Elmer model spectrometer (LAMBDA XLS) at 276 nm, taking aliquots of 250  $\mu\text{L}$  every 15 min throughout the EC process and dissolving the aliquots of  $\text{WO}_3$  in 5 M  $\text{H}_2\text{SO}_4$ .

The  $^{187}\text{WO}_3$  was prepared by irradiation with thermal neutrons of 100 mg of  $\text{WO}_3$  in the ININ Triga Mark III nuclear reactor. Irradiation was performed in the SINCA system of the nuclear reactor for 3 min at a neutron flux of  $1.4 \times 10^{14}$  neutrons / s  $\text{cm}^2$ , giving a specific activity of 1.8  $\mu\text{Ci} / \text{mg}$  of W-187. The process of removal of the  $^{187}\text{WO}_3$  surface contamination, by the electrochemical methods studied, was determined by a gamma spectrometry system, consisting of a coaxial GeHp CANBERRA detector connected to a CANBERRA 2002CSL preamplifier, a CANBERRA 3105 high-voltage power supply, a Tennelec TC 243 amplifier and a CANBERRA multichannel analyzer supported by Maestro software. Samples (steel specimens, electrolytic solution and precipitates) were quantified for 900 s, at an energy of 134.82 KeV, corresponding to the W-187. The uranium contained in the stainless steel specimens was determined with an Eberline SMR-200 monitor attached to an HP-100 detector and gamma-spectrometric electrolytic solutions based on the 92.6 or 1001 KeV gamma ray peaks corresponding to Th-234 or Pa-234m, daughters of U-238 [5].

## 2.3. Determination of fundamental parameters of the electrochemical process

The pH and potential to be used in the electrocoagulation (EC) method were determined by cyclic voltammetry and chronoamperometry, following the procedure described below. Cyclic

voltammetries as a function of pH were performed in an Epsilon potentiostat, using W-EPA |A, pure iron (Fe) and Ag |AgCl as working electrode, counter-electrode and reference electrode, respectively, where A refers to type 304 stainless steel. Tests were performed at 100 mV / s at 24 °C, in a potentiostatic cell with a capacity of 10 mL, with stainless steel plates of 3 x 0.5 cm as working electrodes. The pH of the carrier electrolyte was adjusted with concentrated H<sub>2</sub>SO<sub>4</sub> and 1M NaOH and measured with a HI 2550 pH / ORP digital potentiometer. All tests were performed in duplicate. From the voltammetric tests, the pH was chosen with the largest potential operating window. At this pH, the chrono-amperometric tests were performed in duplicate, applying different potentials, from 800 to 2800 mV for 5 min to complete 120 min, with constant agitation at 800 rpm and 24 °C, using as anode W-EPA |A and as cathode Fe. Plots (current vs time) were constructed to determine the potential of the higher current. The wear of the working electrode was determined by gravimetry, i.e., the electrode was weighed before and after each process.

## 2.4. Electrocoagulation

In order to determine the best conditions for removal of U in stainless steel by electrocoagulation, three parameters were studied: the anode / cathode distance, the type of cathode material and the anode / cathode arrangement in the electrochemical cell. These tests were first performed with W-EPA specimens as describe in the following sections, and then applied the best conditions on the U-EPA specimens.

### 2.4.1 Removal of W on stainless steel plates

**Effect of anode / cathode distance.** The anode (W-EPA |A) / cathode (Fe) distance was evaluated to determine the best conditions for removal of WO<sub>3</sub> from the surface of the electrodes in an acrylic rectangular cell of 16 x 4 x 5 cm. Separation distances were tested from 1 to 5 cm anode-cathode, as reported in the literature [3, 6], under predetermined pH and potential conditions. The concentration of WO<sub>3</sub> in the solution was monitored by UV-Vis spectrophotometry, and the weight of the W-EPA |A electrodes was recorded before and after the electrochemical process. All tests were performed in duplicate.

**Effect of the counter electrode material.** Four types of counter electrode materials, Ti, Fe, Al and C, were evaluated in order to obtain the highest efficiency of the electrocoagulation process

[6-7]. For these tests, 3 x 0.5cm type 304 stainless steel plates (304), coated with WO<sub>3</sub> in polyacrylate (W-EPA |A), were used as anodes at the predetermined pH, potential and distance conditions and as counter electrodes (cathodes) plates of 3 x 0.5 cm. The parameter, sludge generation at the end of the EC process (LW), was evaluated. The electrolytic solution was filtered with filter paper, and the precipitate was dried in the oven at 105° C for 10 min, allowed to cool in a desiccator and then weighed to obtain the weight of the sludge. Each test was performed in triplicate.

**Effect of the circular arrangement of the electrochemical cell.** Eight anode / cathode pair configurations were studied. The anode was a 0.5 cm diameter steel rod coated with W-EPA |A and the cathode a Ti grid in cylindrical form. Both electrodes had a height of 6 cm. The W-EPA |A anode was placed in the center of the Ti cylindrical mesh, as shown in Figure 1A. The effect of the anode / cathode distance was studied, varying the cathode meshes diameter from 1 to 8 cm. The conditions previously determined for pH (1), potential (2.4V), support electrolyte (0.1 M H<sub>2</sub>SO<sub>4</sub> at pH = 1 adjusted with 1M NaOH) and contraelectrode (Ti) material were used. The tests were performed in triplicate, and the concentration of WO<sub>3</sub> in the solution was monitored by UV-Vis spectrophotometry.

**Distribution of W in the electrochemical system after the EC process.** The distribution of W in the different parts of the electrochemical system (cathode, anode, electrolytic solution and sludge) after applying the EC process, was studied. The electrocoagulation process was performed using, as anode, a <sup>187</sup>W-EPA |A plate and maintaining the previously determined conditions: support electrolyte 0.1M H<sub>2</sub>SO<sub>4</sub> at pH = 1, cell potential 2.4 V, anode / cathode distance of 1 cm and Ti counter electrode. The W-137 activity contained in the anode (before and after the process), cathode and electrolytic solution and the precipitate formed at the end of the process was determined by gamma spectrometry.

#### 2.4.2. Removal of uranium from stainless steel

Two configurations of electrochemical cells were tested with the objective of evaluating the efficiency of removal of U in each array: a rectangular one with dimensions of 16 x 4 x 5 cm and a volume of 150 mL, and a circular one of 5.5 cm of radius with a volume of 1000 mL (Figure 1) both were made of lab grade acrylic. The EC conditions were as follows: support

electrolyte 0.1 M H<sub>2</sub>SO<sub>4</sub> at pH = 1, 2.4 V and Ti counter electrode. The tests in the rectangular cell configuration were performed in duplicate, and in the circular cell configuration, in triplicate.

#### **A) Anode / cathode arrangement face to face**

A configuration of 3 anode / cathode pairs, being the anode U-EPA |A and the cathode Ti (See Figure 1B), was studied. The anodes were consecutively placed to the left side of the cell, connecting to the source's positive terminal and the cathodes on the right side, connected to the source's negative terminal. The distance between electrodes was set at 1 cm.

#### **B) Alternate anode / cathode arrangement**

A configuration of 4 anode (W-EPA |A) / cathode (Ti) pairs, were placed consecutively inside the cell, connected all the anodes to the source's positive pole terminal and the cathodes to the negative, as shown in Figure 1C. The distance between cathode / anode and between electrode pairs was 1 cm.

#### **C) Anode / circular cathode arrangement**

In the circular arrangement, the U-EPA |A anode of cylindrical shape was placed in the center of the cell at 2 cm of distance from the cathode, which was a Ti mesh of 4 cm in diameter (the optimal diameter found during the W-Ti mesh test cycle) see Figura 1A. The U activity at the anodes was determined before and after each process, as described in section 2.2.

### **2.5. Decontamination of radioactive wastes of noncompactable materials contaminated with uranium.**

The best conditions determined in the test studies of the EC for removal of W and U in stainless steel plates were used in the decontamination process of two actual metal pieces contaminated with uranium, classified as radioactive waste. The pieces were first modeled in Solidworks CAD software to track effectiveness of the decontamination process. Levels of part contamination were noted in the models (by letter) before and after the electrocoagulation



decontamination process to study its effectiveness on real parts in the nuclear industry, see Figure 2.

The contaminated piece, designated "1" here, is a stainless steel ball valve 8 cm long by 7 cm in height. It was necessary to disassemble it to facilitate decontamination. The contaminated piece, here numbered "2", is a 0.7 cm thick stainless steel bypass connector with four 5 cm (internal diameter) openings that has overall dimensions of 9.5 by 7.5 cm weighing 990g. The CAD drawings of both pieces were marked (by letter) in various areas, in order to monitor contamination levels before and after the decontamination treatment.

### 2.5.1. Determination of pollution levels of actual contaminated parts

Before and after decontamination treatment the pieces' contamination levels were tested with the Eberline SRM-200, taken in two replicates. Both external and internal smears of the test pieces were obtained, in order to determine if the contamination in the piece was fixed or mobile. The smears were moistened in 50% Bx-40 decontaminant and quantified on the Eberline SRM-200 monitor. The contamination levels (NC) were calculated for each zone using equation one (1) [8]:

$$NC = \frac{cps_s - cps_b}{A \varepsilon_d \varepsilon_s} (1)$$

Where  $cps_s$  = counts per second of sample,  $cps_b$  = counts per second of the background,  $A$  = contaminated area in  $cm^2$ ,  $\varepsilon_d$  = detector efficiency (0.4819),  $\varepsilon_s$  = smear trailing efficiency (0.17), which was determined experimentally [8]. It was difficult to assess the fixed contamination on either the inside or the outer surface of the pipe [9].

### 2.5.2. Application of the EC process to actual pieces contaminated with U

The electrocoagulation decontamination treatment by electrocoagulation of the two U-contaminated pieces was carried out under the following conditions: circular arrangement, cell

potential of 2.4 V, electrolytic solution of 0.1 M  $\text{H}_2\text{SO}_4$  at pH = 1, cathode in Ti mesh form and 1 h of process time. The mesh circular arrangement was selected in this work, since it avoids the distribution of uneven current within the process while increasing the active sites and allows the process to be used for pieces of different geometries and shapes.

In the case of piece 1, the treatment was separately applied to the two parts of the previously dismantled valve: the valve stem and housing. The electrochemical cell was sized 500 mL for the stem and 1 L for the housing (anodes). These components (as anodes) were placed at the center of the cell and the cylindrical Ti mesh of 4.5 cm in diameter x 6.0 cm high cathode, (in the case of the stem) and 8.5 cm diameter x 5.5 cm (for the housing) encircling the anode. The anode-cathode distance was approximately 2 cm. The process had a constant magnetic stirring of 600 rpm and the total volume of supporting electrolyte was 200 mL and 500 mL for the stem and the housing respectively (Figure 1A).

For piece 2, the connector (anode) was mounted to the center of the 2 L cell, and around this was a Ti (cathode) mesh 11 cm in diameter x 12 cm in height. The total volume of carrier electrolyte was 1800 mL (Figure 1A). At the end of the EC treatment, Both pieces were monitored with the Eberline SRM-200 detector, using externally and internally smears [9]. The cathodes, the filtered sludge resulting from the EC process, and the supporting electrolyte from each test were also analysed after treatment using gamma spectrometry [5].

### 3. Results and discussion

#### 3.1. Electrochemical system

The largest potential window, i.e., the highest I / E ratio of the electrochemical system under study, was obtained at a pH of 1. It was found that at pH of 14 the system required a higher current to reach a small potential due to the formation of oxides on steel surfaces, corresponding to the chemistry of solutions of this material as a function of pH [10, 11]. Therefore, to enhance effectiveness of the treatment, the pH selected to carry out the electrocoagulation was 1. This pH was obtained by addition of some  $\mu\text{L}$  of 1M NaOH to a solution of 0.1 M  $\text{H}_2\text{SO}_4$  [11].

Figure 3 shows the charge variation (Q) and the mass wear at the anode as a function of the potential (E) using the pH 1 electrolytic solution. The load (Q), due to the mass transport,

increases slightly from 1 to 5 C until reaching an  $E_{\text{cell}}$  of 1.6 V, and, at higher potentials, the load increases significantly from 5 to 30 C until reaching a maximum at  $E_{\text{cell}} = 2.6$  V.

The anode mass wear (W) increases as the  $E_{\text{cell}}$  increases; between 0 and 1.6 V, the wear is nearly asymptotic, at  $E > 1.6$  V, W increases continuously (See Figure 3). Even when the anode continues to wear out at  $E_{\text{cell}} > 2.4$  V, the generated load is practically the same ( $Q = 30\text{C}$ ) so that using potentials greater than 2.4 V does not improve the mass transport of the process but would increase energy consumption. Therefore, the team selected the use a potential of 2.4 V for subsequent studies [11].

### 3.2. Electrocoagulation

The working conditions used in these studies were: 0.1 M  $\text{H}_2\text{SO}_4$  solution at pH = 1 and a potential of 2.4 V.

#### 3.2.1. Effect of electrode distance on $\text{WO}_3$ removal

The mass of  $\text{WO}_3$  removed by the electrocoagulation process as a function of the anode (W-EPA |A) / cathode (Fe) distance is shown in Figure 4. The greatest removal of  $\text{WO}_3$  (0.7 mg) from the W-EPA |A anode was obtained when the anode and cathode were located 1 cm apart. The decreasing behavior can be modelled by a function of the type  $R = -0.185 + 1.189e^{(-0.269*d)}$ , with an R-squared of 0.9996, where  $R = \text{WO}_3$  removed, and  $d = \text{electrode distance}$ . As the distance between the electrodes increases, the removal declined because the added distance influences the resistance to the passage of the current [3,10]. Therefore, 1 cm distance between anode / cathode was observed to perform the best and was selected for the rest of the tests when determining the best conditions of W. removal with other variables.

#### 3.2.2. Effect of the counter electrode material on the removal of $\text{WO}_3$

The generation of sludge (LW) after 1 h of the EC process was the parameters evaluated during the tests with the various cathode materials studied. Figure 5 shows the variation of LW as a function of the type of cathode used in the EC process. The largest mass of sludge generated (36 mg), after 1 h under the EC process was obtained using Ti while the lowest sludge generation (24 mg) when found using C. These results can be explained by the fact that oxides

and hydroxides of titanium increase their solubility in reducing medium therefore, the concentrate non-oxidizing acids as  $\text{H}_2\text{SO}_4$  cause a dropping of the Ti potential [12]. Thus, Ti cathode can accelerate the corrosion of W-EPA | Fe electrode, and consequently increase its dissolution without affect the Ti in most cases, due to formation of a very stable titanium hydride film. This film allows the production hydrogen on its surface that is proportional to the galvanic current flow [13]. The produced hydrogen can rise and generate a flow able to remove the flocs that contain  $\text{WO}_3$  from the surface of the anode W-EPA | Fe during the EC process, that sediment in the sludge [3, 6, 14].

In contrast, the lowest sludge generation during the EC of  $\text{WO}_3$  in presence of the C counter electrode and W-EPA | Fe electrode, is caused by the decrease of the hydrogen production in the system (which facilitates the removal of  $\text{WO}_3$  adhered to the anode W-EPA | Fe during the EC process), as result of the overlap in the stability electrochemical of carbon and the electrochemical reactions involving water to form  $\text{H}_2$ , [15]

According to the results and the discussion showed before, Ti is the most appropriate material to be used as a counter electrode (cathode) in the EC process, thus it was selected as a cathode for the remaining tests. A second alternative is Al, sludge generated with the Al acting as the cathode were only slightly lower than those of Ti [3,7,16,17]. The team selected a Ti cathode for further testing, however, because the current applied during the process favors the electric field, and therefore the production of metal ions in the solution to interact with  $\text{WO}_3$ , when compared to aluminum as a cathode.

### 3.2.3. Effect of electrochemical cell arrangement on the removal of $\text{WO}_3$

In the design of electrocoagulation cell, the position of the electrodes in the reactor can be optimized as a function of hydrodynamic parameters, current density, electrode gap and operating conditions on voltage [18]. In this way, the intensity of the electric field varies proportionally with the distance from the electrodes, which at a distance smaller the intensity increases as Figure 6 shows the percentages of  $\text{WO}_3$  removed by the EC process in the anode / circular cathode array, where the highest recovery percentage of  $\text{WO}_3$  was obtained using a Ti (cathode) mesh with a 2 cm radius.

In general, in a circular arrangement, the current density distribution is uniform; however, it is evident that, at anode / cathode distances less than and greater than 2 cm, rate of  $\text{WO}_3$  removal decreases. When the electrodes are separated, the resistance increases, current decreases and the potential becomes variable. In contrast, when the electrodes are closer, the resistance decreases, the current increases by the  $\text{WO}_3$  removed just to 2 cm and the voltage is constant [3,19].

In this sense, the circular cell configuration was chosen for the decontamination of the actual contaminated parts, since it offers quantitative potential with geometric flexibility when decontaminating parts of diverse size and shape taken from an actual reactor in the field.

### **3.2.4. Distribution of W in the electrochemical system after the EC process**

In order to quantitatively determine in which phases of the EC processes the W is recovered, the electrolytic solution, the sludge, the anode and the cathode were all tested with the W-187 radiotracer using the previously established EC conditions (2.4 V, 0.1 M  $\text{H}_2\text{SO}_4$ , Ti cathode and 1 h of process). The removal efficiency of W-187 at the anode was 88.93%; 11.07% remained attached to the anode, while 86.93% of the W-187 was recovered in the sludge, 1.65% in the electrolytic solution and 0.35% in the cathode.

In the process of EC, the anode is known to be the sacrificial electrode that dissolves, forms metal ions and hydroxyl ions, producing a precipitate of iron hydroxide, which carry the contaminants away. This mechanism was the same as observed during the team's tests as the highest percentage of W-187, at the end of the EC process, was found in the sludge [3,7,14].

### **3.2.5 Removal of U by electrocoagulation**

The best conditions for the removal of  $\text{WO}_3$  by electrocoagulation, i.e., 2.4 V potential, 0.1 M  $\text{H}_2\text{SO}_4$  at pH = 1, Ti cathode and 1 h process time, were then applied to stainless steel plates contaminated with  $\text{UO}_2(\text{NO}_3)_2$  bound in EPA (anode), in four electrochemical anode / cathode (A/C) cell arrays: (1) an A/C pair face to face, (2) three A/C pairs face to face, (3) four A/C pairs alternating and (4) an A/C pair, whose anode is a cylinder and the cathode a cylinder mesh surrounding the cathode offset by 2 cm.

Figure 7 presents the percentages of U removal in the (A/C) face-to-face and alternating configurations. In the case of the face-to-face configuration, the flow of electrons follows a line, and there will be a greater resistance to the passage of the current [6, 7, 19]; thus, the percentage of U removed from the steel plate depends on the anode / cathode distance (A/C). At the smallest A/C offset distance greater removal of U was observed. It is, therefore, recommended that the A/C offset distance be less than 2 cm, using up to two anodes per array to removal more than 80% U.

In the alternating arrangement, the removal of U is similar in each of the four A/C pairs; on average, 77.8% of U is removed in each A/C pair, and the resistance to the current passage is lower than in electrodes arranged face to face. In this case, the current is divided between all electrodes with the same voltage [19]. In the ‘alternating arrangement’, it should be feasible to change (decrease or increase) the number of A/C pairs without significantly affecting the percentage of U removed by the EC process. However, if the electrochemical array only has a single A/C pair, the percentage of U removal is approximately 95%. These results clearly show that increasing the number of A/C pairs in the electrochemical arrangement, either arranged face-to-face or in the alternating configuration, lowers the percentage of U removed from the anode stainless steel plate in the EC process by 18% (alternating arrangement) and from 15% up to 40% in the face-to-face arrangements, depending on the number of A/C pairs contained in the electrochemical cell. That is, the presence of several A/C pairs in the same electrochemical cell has an anti-synergistic effect, which was most notable in the face-to-face arrangement.

On the other hand, using the circular A/C configuration removes 91.4% of the U on the stainless steel rod, a percentage similar to that obtained in the face-to-face arrangement using a single A/C pair. However, the face-to-face configuration can only be used on plates, while the circular arrangement, even though it removes slightly less U, provides greater flexibility in the geometry of the parts that can be decontaminated. It assures better agitation thus making the process more homogeneous while the circular arrangement (in cathode mesh form) avoids process dead spots by increasing active sites. In conclusion, if the piece to be decontaminated is a plate, it is recommended that decontamination by EC at 1cm A/C distance should be employed, but if the piece is irregular the team suggests that decontamination be performed EC with a circular cathode with approximately a 2 cm A/C offset.

The decontamination process of stainless steel by EC consists of the following steps (See Figure 8): at first, iron ions are generated in situ by electrolytic oxidation of a sacrificial anode (contaminated metal) triggered by an electric current applied through the electrodes, and, at the cathode (Ti), water is reduced into hydrogen gas and hydroxyl anions [3,7,14]. The iron ions generated by electrochemical dissolution of the sacrificial anode tow the uranyl ions attached to the stainless steel and form hydroxides by precipitation. It is also possible that uranyl ions are able to be adsorbed on iron hydroxides [20,21]. Thus, the uranyl ions detached from the metal surface by electric current applied through the electrodes are removed and precipitate as hydroxides that settle on the bottom of the cell [20].

### **3.4. Decontamination of radioactive wastes of noncompactable materials by EC.**

Contaminated pieces numbered 1 and 2 (Figure 2) were first inspected to define their levels of internal and external surface contamination. Following this initial characterization the EC process was performed and the efficiency of decontamination was evaluated.

#### **PIECE 1**

The surface contamination levels of Piece #1 were determined directly by both external and internal smears in two cycles. The smears were taken in 8 lettered areas, shown in Figure 9A, where the respective contamination levels (NC) are designated. It took at least 3 smears, two before EC treatment to establish initial NC levels, and a final one after decontamination.

Because of their complex shapes, the contamination levels of some zones on the piece could not be easily measured, for example at the C point in the piece. By this raison swears were obtained in all piece, and the contamination levels were only recorded in Bq. The external surface of the piece was decontaminated after the second swear. All the pre-process smears from inside of pieces showed higher levels of contamination, upper the background (at the internal point C). Consequently, to verify the internal contamination levels, the piece was disassembled as shown in Figure 10.

The seven parts that make up Piece #1 were monitored both directly and by local smears. The only contaminated components were B (valve stem) and C (body) shown in Figure 10. Smears

were again taken, in two stages pre-processing, to determine if the contamination was fixed or removable. The initial contamination level of the stem was 1232 Bq, then the second smears showed 653 Bq indicating that much of the initial contaminates were easily removal as non-adhering substances (See Figure 9B). Finally, after the EC process, smears showed only 62 Bq, indicating that 90% of adhering surface contamination was removed by the EC process. As the approximate area of the stem of 25 cm<sup>2</sup>, its NC is of 2.48 Bq/cm<sup>2</sup> after EC treatment.

In the case of the valve body shell (See Figure 10 part C), the initial levels of internal contamination ranged from 380 to 5800 Bq, and after applying the EC process, they fell to between 277 and 2927 Bq; thus using the estimated internal surface of 30 cm<sup>2</sup>, NC is between 19.23 and 97.57 Bq/cm<sup>2</sup>. As seen, the average percentage of uranium removal from the shell was only 50%. It is important to note that when taking the smear samples the presence of grease inside the shell was observed. The exemption limits for the recycling of metallic waste, marked by NOM-035-NUCL-2013, establish a maximum value of surface contamination of the piece of 1 Bq/cm<sup>2</sup> for the case of natural uranium [22,23]. As reported, the NC of the valve stem and body, after the EC process, are greater than this standard limit, so these parts could only be reused in already contaminated areas [23].

## PIECE 2

The geometry of Piece #2 made it possible to directly determine contamination level of the workpiece prior to smearing and the EC process. Figure 11A shows the division into zones of Piece #2 and Figure 11B the contamination levels (NC) in Bq /cm<sup>2</sup> of these zones: initial, after the first smear, after the second smear and after EC. The NCs of the second process obtained after the EC process were on average less than 1 Bq /cm<sup>2</sup> (Figure 11B); therefore, this part can be dispensed unconditionally for unrestricted reuse in any work area, based to the limit established by NOM-035-NUCL-2013. In this case, 98% of the uranium was removed from the piece by the EC process.

Natural uranium is composed of three isotopes, U-234 (2,455x10<sup>5</sup> y), U-235 (7,038x10<sup>8</sup> y) and U-238 (4,468x10<sup>9</sup> y), that emit alpha particles as their primary radiation. Direct monitoring of alpha activity is not easy in irregular pieces, so the use of smears allows access to contaminated areas where it would be impossible to place conventional detectors close enough to the surface, including curved surfaces, such as the inside and outside of pipes or pumps.



While, direct measurement detects both fixed and loose contamination whereas smears measure only “loose” contamination. On the other hand, the fraction of removable contamination picked up on a smear on of a dirty or greasy surface is difficult to quantify precisely [9], as is the case of the casing of Piece #1. Smears from these parts included grease from the parts interior, even after the EC process. Therefore, only 50% of the uranium could be removed from this piece, whereas, for Piece #2, whose surface had no grease, the EC process was able to remove up to 90% of the uranium contamination. The surface condition of the part is a fundamental issue during decontamination using the EC process. The presence of grease or oily dirt/dust decreases the efficiency of the electrochemical process, so it is recommended that the surface be free of grease and oily dirt/dust before electrochemical treatment to improve decontamination efficiencies.

The estimation of contamination levels through direct monitoring of the piece is the most accurate method to determine the fixed and removable contamination of the piece. However, when the contamination occurs on irregular surfaces or on the inside surfaces of a workpiece, direct monitoring is infeasible and smears should be used. It must be noted, however that a smear only provides information on the removable contaminants, but it can provide a reference for total contamination levels of the piece allowing the facility manager to make decisions related to disposal processes of used equipment.

#### 4. CONCLUSIONS.

The EC process can be an effective means to remove up to 90% of the uranium contamination present in cylindrical pieces of stainless steel, with contaminated steel parts:  $\text{UO}_2(\text{NO}_3)_2 \cdot 6\text{H}_2\text{O}$ , acting as an anode, under the following conditions: electrolytic solution of 0.1 M  $\text{H}_2\text{SO}_4$  at pH = 1,  $E_{\text{cell}} = 2.4 \text{ V}$ , 1 h of process and cathode in the form of Ti mesh, under a circular arrangement successful results at this level of removal were observed. These processing conditions were obtained from tests carried out, first with stainless steel plates contaminated with tungsten oxide, considering that the W is an element with chemical properties analogous to U, and later confirmed with materials contaminated with uranium. These conditions were then applied to actual radioactive waste. Two pieces, of irregular geometry, that had been contaminated with U, were tested as the anodes in the electrochemical test lab.

The EC process was found to be a feasible solution for the decontamination of U-contaminated steel metal parts. Using the conditions determined by the research team, it was possible to remove up to 90% of the U contamination and to reclassify certain products for unrestricted use. However, the presence of grease and oily dirt/dust on the surface of the parts reduced the efficiency of electrochemical treatment, so it is recommended that grease and oily dirt/dust be cleaned from workpiece surfaces prior to treatment by the EC process. The geometry, dimensions and surface conditions of the metal parts to be decontaminated by the EC process directly influence the removal efficiency of the contaminant present in the part.

The removal process of uranium attached to stainless steel (decontamination) by electrocoagulation (EC) is done through the application of an electric current between the contaminated metal (sacrificial anode) and the cathode (Ti) in an aqueous medium. The anode is dissolved, towing uranyl ions to the solution and forming a precipitation of iron and uranyl hydroxides.

#### **ACKNOWLEDGMENT.**

This research was supported by ININ Grant DR-004. We thank Dr. David Lizcano for supplying the contaminated pieces and the students O. D. Esquivel Mejía and J. E. Hernández Cruz for their assistance in this work. A.A. Pujol Pozo thanks the (CONACyT) for the master's degree in Environmental Engineering awarded for the development of this research topic as well as the Center for Research and Technological Development in Electrochemistry SC and the National Institute of Nuclear Research of Mexico for the stay in both institutions.

#### **5. REFERENCES.**

- [1] L. Noynaert, Decontamination processes and technologies in nuclear decommissioning projects, in: M. Laraia (Ed.), Nuclear Decommissioning: Planning, Execution and International Experience, Woodhead Publishing Series in Energy, U.K., 2012, pp. 319–345.
- [2]. S.L. Voit, S.T. Boerigter, An analysis of radioactive waste minimization efforts at Los Alamos National Laboratory, Technical Report LA-UR-98-150, Los Alamos National Laboratory, USA, 1997, pp-98-150.

- [3]. S. Garcia-Segura, M. Maesia, S.G. Eiband, J. Vieira de Melo, C.A. Martínez-Huitile, Electrocoagulation and advanced electrocoagulation processes: A general review about the fundamentals, emerging applications and its association with other technologies, *J. Electroanal. Chem.* 801 (2017) pp. 267-299.
- [4] A. A. Pujol Pozo, Tratamiento electroquímico de materiales no compactables contaminados con compuesto de uranio. Master Thesis, CIDETEQ, Mexico, 2016.
- [5] I.E. Saleh, A.A. Abdel-Halim, Determination of depleted uranium using a high resolution gamma-ray spectrometer and its applications in soil and sediments, *J. Taibah Univ. Scienc.* 10 (2016) pp. 205-211.
- [6] N. Modirshahla, M.A. Behnajady, S. Mohammadi-Aghdam, Investigation of the effect of different electrodes and their connections on the removal efficiency of 4-nitrophenol from aqueous solution by electrocoagulation, *J. Hazard. Mater.* 154 (2008) pp. 778-786.
- [7] O. Sahu, B. Mazumdar, P.K. Chaudhari. Treatment of wastewater by electrocoagulation: a review, *Environ. Sci. Pollut. Res.* 21 (2014) pp. 2397-2413.
- [8] Monitoring for compliance with exemption and clearance levels. Safety Reports Series No. 67. IEAE, Vienna, 2012.
- [9] P.W. Frame, E.W. Abelquist. Use of smears for assessing removable contamination. *Operational Radiation Safety*, 76 (1999), pp S57-S66.
- [10] *Electroanalytical Methods: Guide to Experiments and Applications*. F. Scholz (Ed.) 2th ed., Springer, Germany, 2010.
- [11] Pujol-Pozo, A.A., Monroy-Guzmán, F., Bustos, E., 2018. Advanced oxidation process for the decontamination of stainless steels containing uranium, *J Mater Sci: Mater Electron*. <https://doi.org/10.1007/s10854-018-9229-3>.
- [12] M. Pourbaix. *Atlas of Electrochemical Equilibria in Aqueous Solutions*. NACE International Cebelcor, Brussels, 1974.

- [13] M. J. Donachie Jr., Titanium: A Technical Guide, second ed., ASM International, The Materials Information Society, USA, 2000.
- [14] J.N. Hakizimana, B. Gourich, M. Chafi, Y. Stiriba, J. Naja, Electrocoagulation process in water treatment: A review of electrocoagulation modeling approaches, *Desalination*. 404, (2017), pp 1-21.
- [15] K. Kinoshita, Carbon: Electrochemical and Physicochemical Properties. John Wiley & Sons, Inc., USA, 1988.
- [16] G. Mouedhen, M. Feki, M.D.P. Wery, H.F. Ayedi, Behavior of aluminum electrodes in electrocoagulation process, *J. Hazard. Mater.* 150 (2008) pp124-135.
- [17] D. Mills. A new process for electrocoagulation *Journal-American Water Works Association*, 92 (2000) pp. 34-43.
- [18] Y. Shao, *Electrochemical Cells: New Advances in Fundamental Researches and Applications*. Intech, Croatia, 2012.
- [19] Handbook of Electrochemistry, C. G. Zoski (Ed.), Elsevier, The Netherlands, 2007.
- [20] T.D Waite, J.A Davis, T.E Payne, G.A Waychunas, Uranium (VI) adsorption to ferrihydrite: Application of a surface complexation model. *Geochimica and Cosmochimica Acta*, 58 (1994) pp. 5465-5478.
- [22] S.A. Cumberland, G. Douglas, K. Grice, J.W. Moreau, .Uranium mobility in organic matter-rich sediments: A review of geological and geochemical processes. *Earth-Sci. Rev.* 159 (2016) pp 160-185.
- [23] Norma Oficial Mexicana NOM-035-NUCL-2013: Criterios para la dispensa de residuos con material radiactivo.
- [19] Recommended radiological protection criteria for the recycling of metals from the dismantling of nuclear installations. Radiation protection 89. European Commission, Germany, 1998.

## FIGURE CAPITONS.

**Figure 1.** Electrochemical cell configurations in face-to-face (A), alternate (B) and circular (C), anode (+) and cathode (-) separate of 1 cm ( $\Leftrightarrow$ ).

**Figure 2.** Actual contaminated parts treated by electrocoagulation: (1) valve and (2) connector in Yee.

**Figure 3.** Electrochemical system bias curve and electrode mass wear.

**Figure 4.** Removal of  $\text{WO}_3$  as a function of the anode distance (W-EPA |A) / cathode (Fe).

**Figure 5.** Generation of sludge (LW) according to the type of counter electrode applying the EC process for 1 hour.

**Figure 6.** Efficiency of removal of  $\text{WO}_3$  by EC as a function of the anode / cathode arrangement type.

**Figure 7.** Efficiency of removal of U by EC as a function of the electrochemical cell configurations, in face-to-face (A) and alternate (B).

**Figure 8.** Mechanisms of U decontamination by electrocoagulation process.

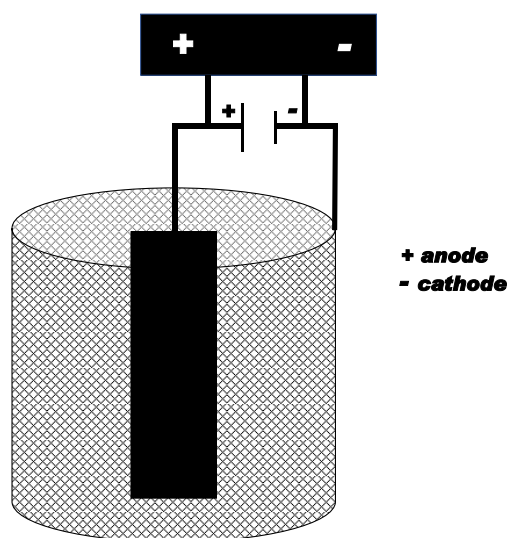
**Figure 9.** Division into zones of Piece #1 (A) and Contamination levels of Piece #1 in Bq during the decontamination process (B).

**Figure 10.** Contaminated piece 1 disassembled into parts: handwheel (A1), packing (A2), wing bolt screw (A3), nut (A4), screw (A5), stem (B) and valve housing (C).

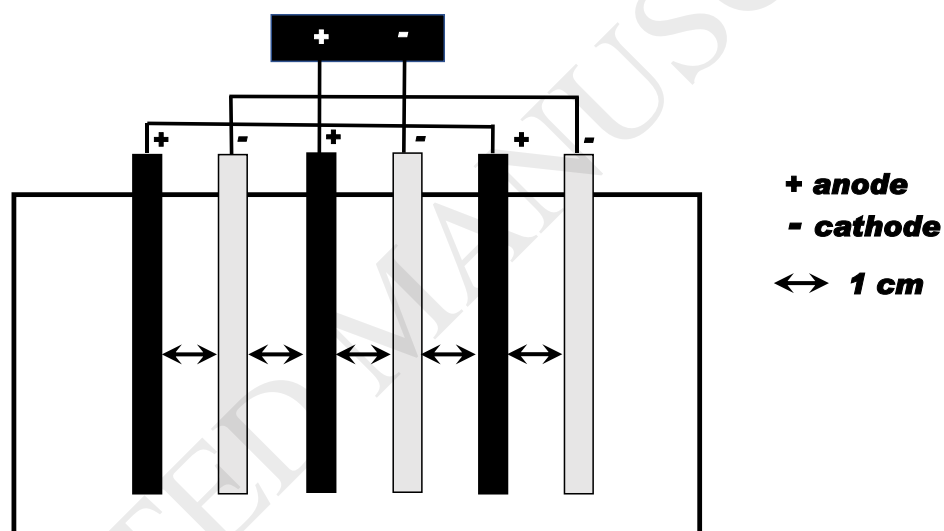
**Figure 11.** Division into zones of Piece #2 (A) and Contamination levels of Piece #2 in  $\text{Bq/cm}^2$  during the decontamination process (B)

Figure 1.

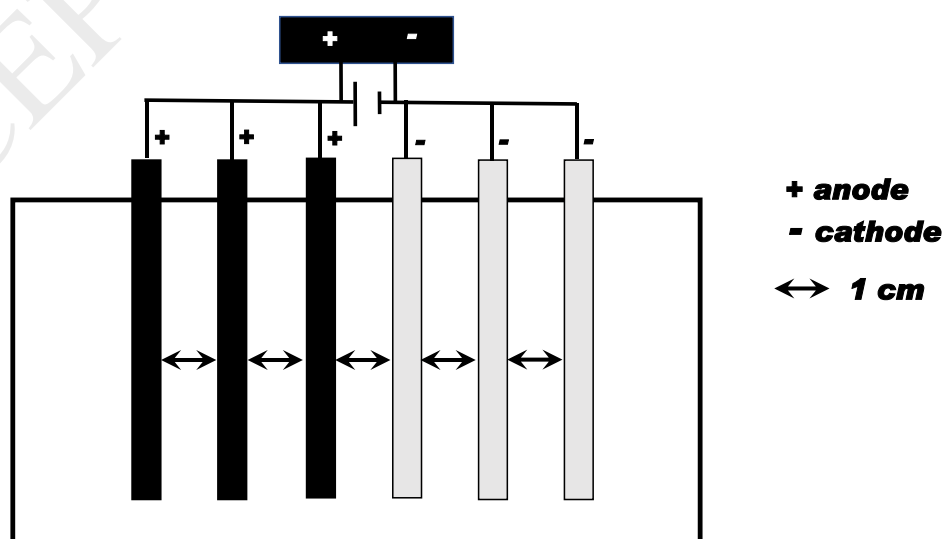
A



B

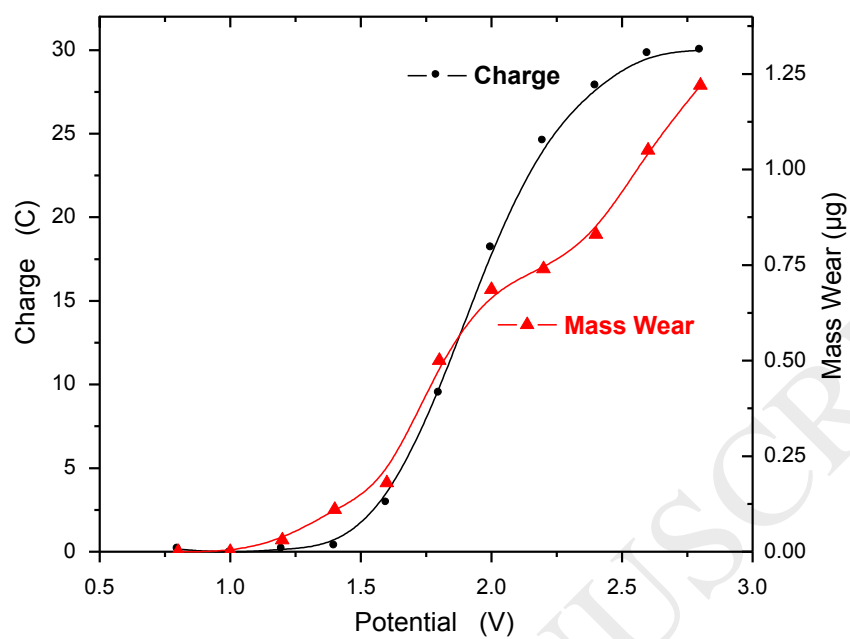


C

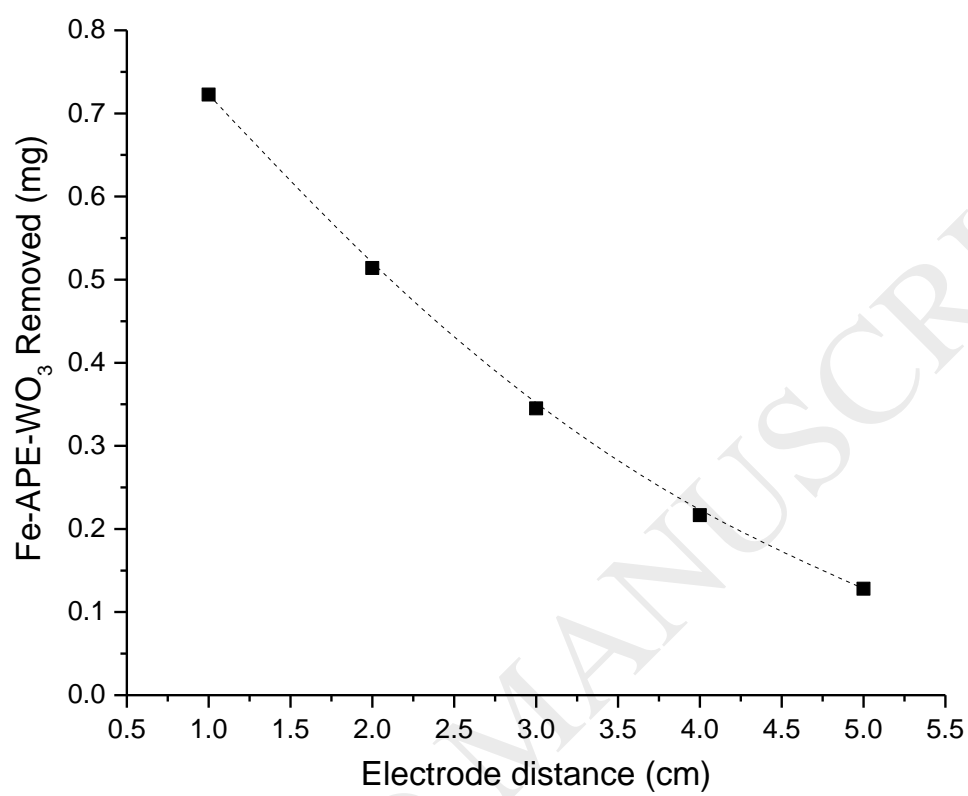


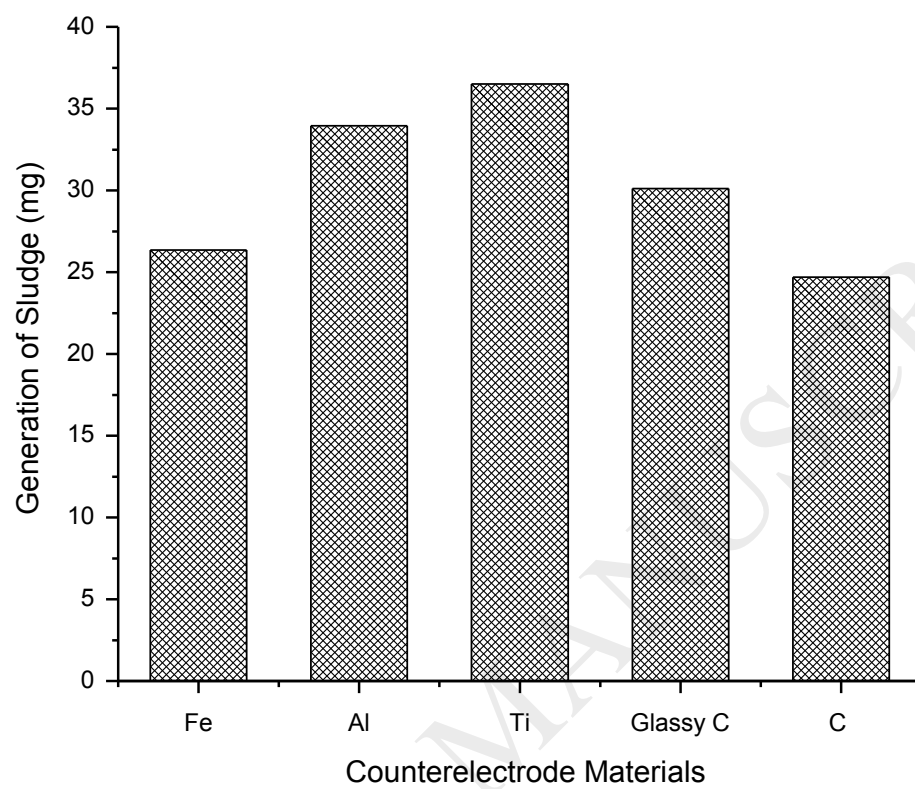
**Figure 2.**



**Figure 3.**



**Figure 4.**

**Figure 5.**

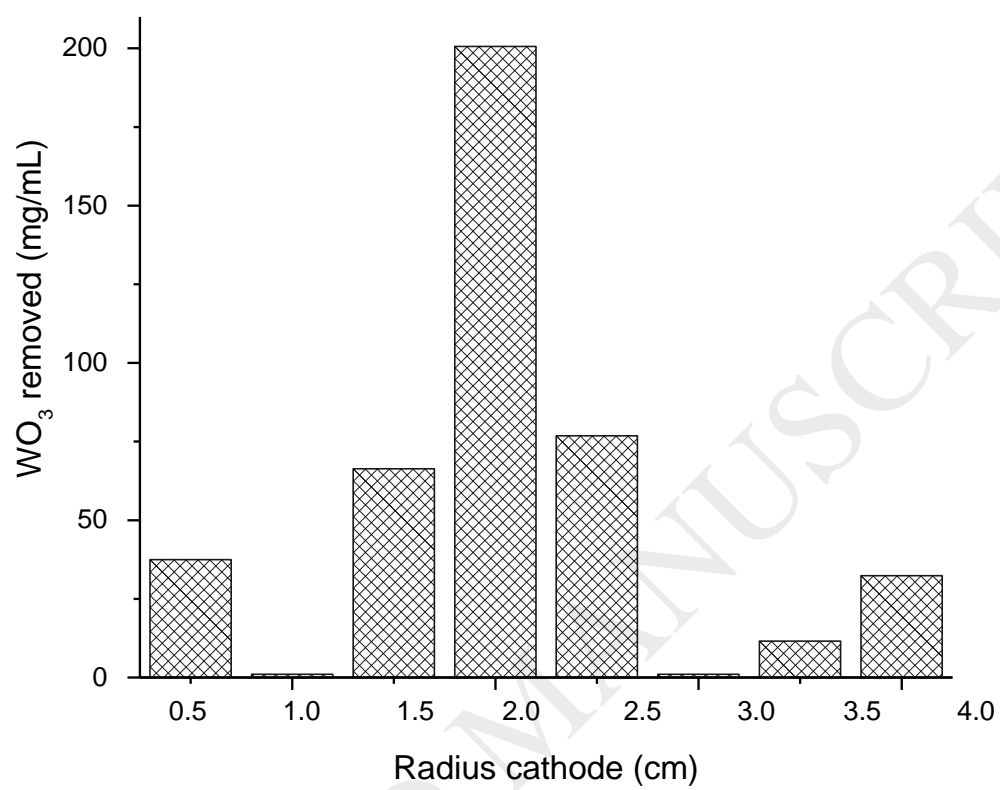
**Figure 6.**

Figure 7.

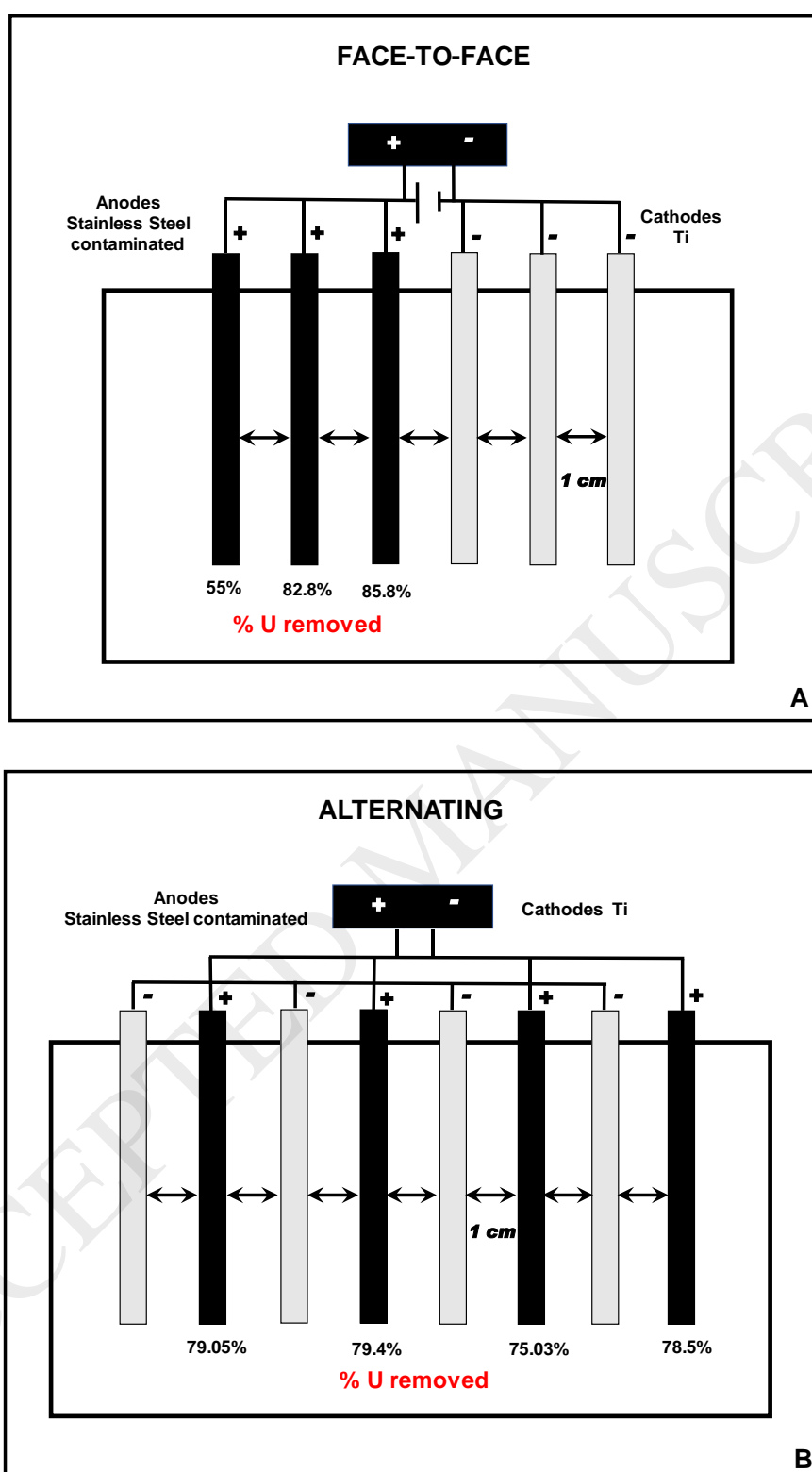


Figure 8.

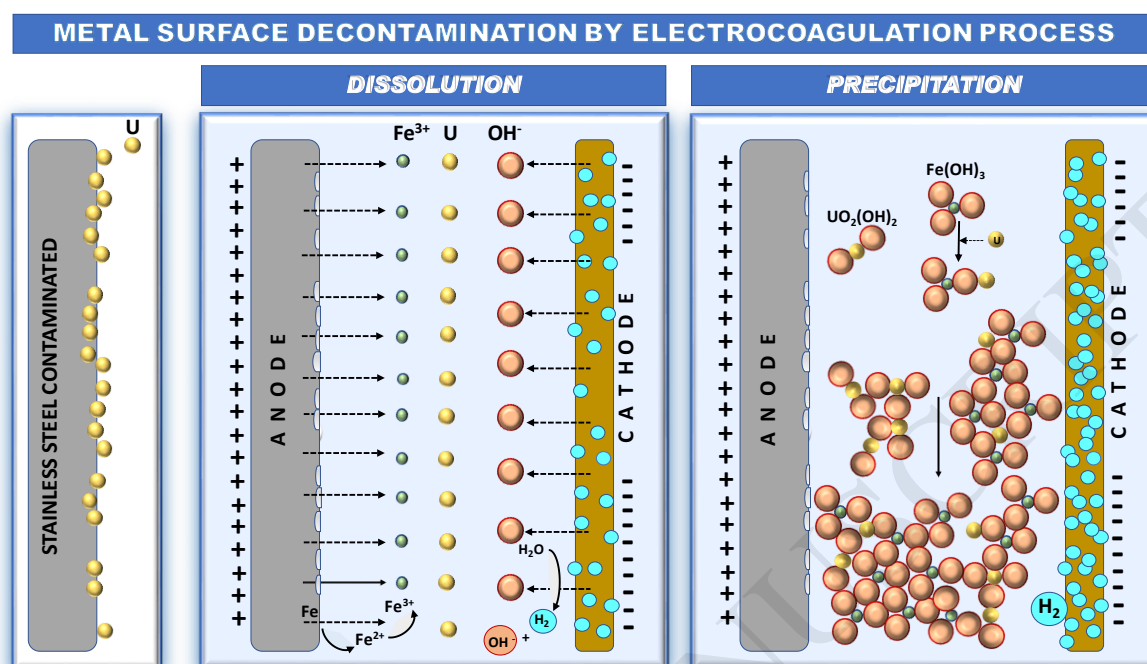


Figure 9.

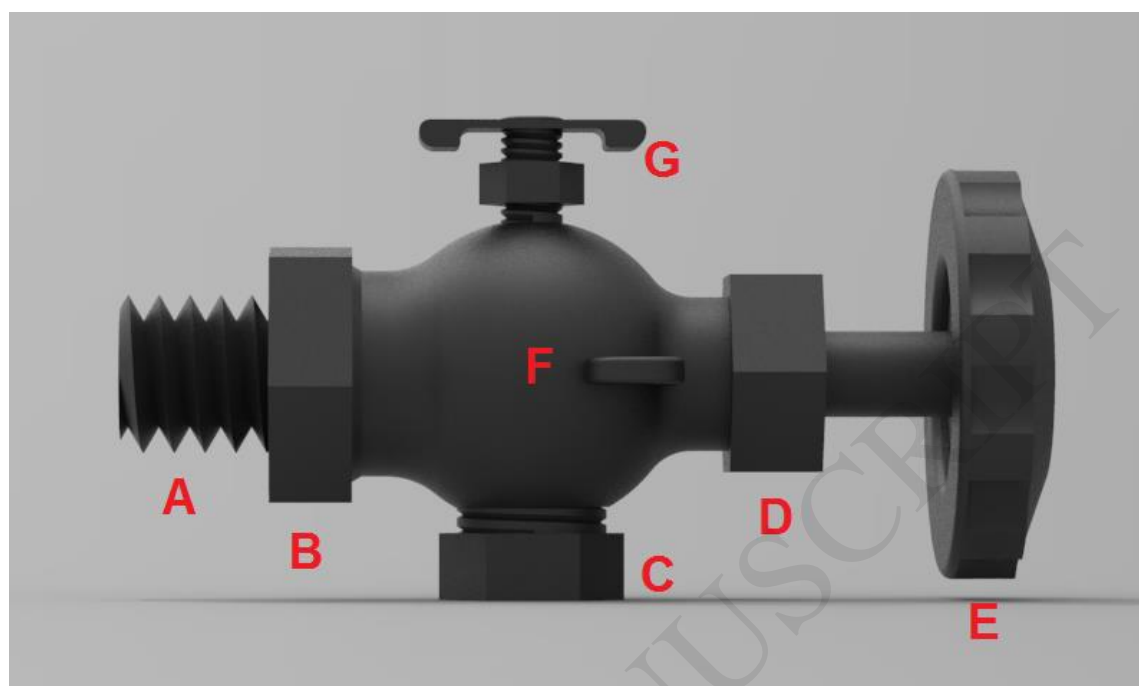
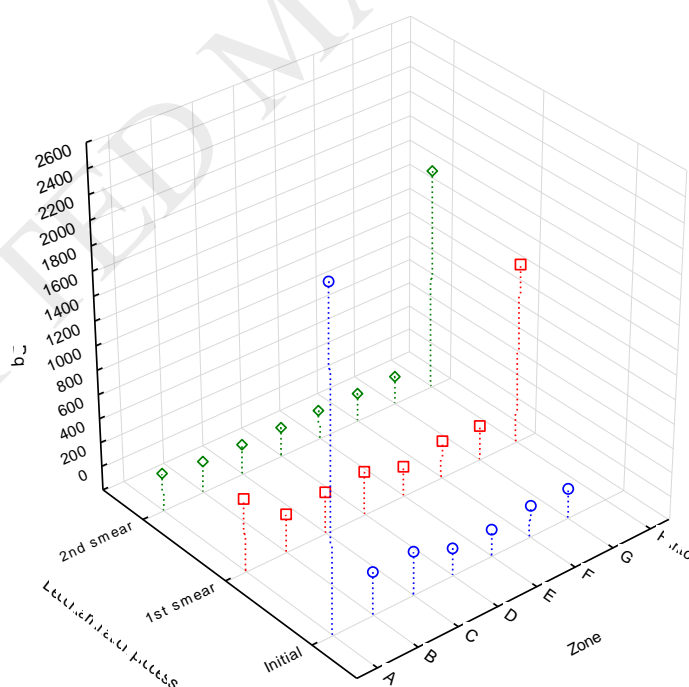
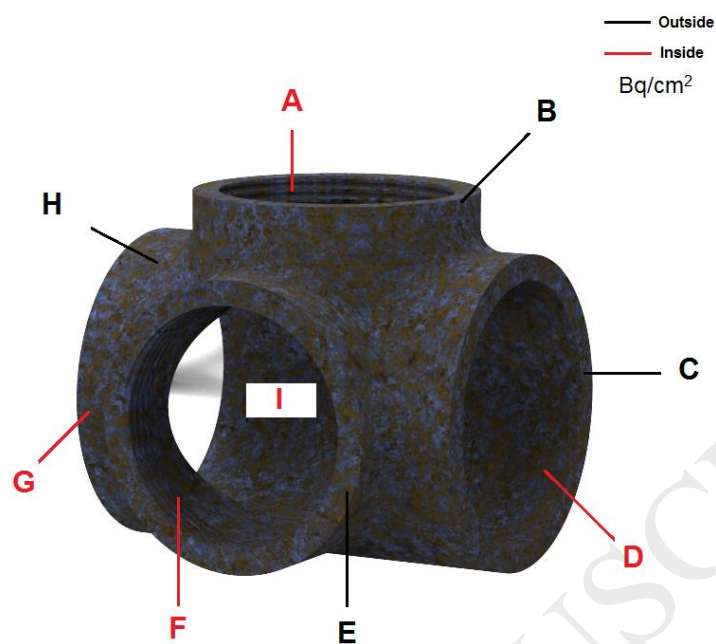
**A****B**

Figure 10.



Figure 11.

**A**



**B**

